

The Southern African Large Telescope (SALT) Calibration System

D. A. H. Buckley^{*a}, J. Brink^a, N. S. Loaring^a, A. Swat^{a,b} and H. L. Worters^a

^aSouth African Astronomical Observatory, Observatory, Cape Town, South Africa

^bEuropean Southern Observatory, Garching, Germany

ABSTRACT

This paper presents details of the instrument calibration system employed on the SALT. It is designed to inject light into the Spherical Aberration Corrector at about the position of the primary mirror caustic, thereby simulating the same degree of vignetting as experienced by celestial objects. A light-shaping diffuser screen, coupled with Fresnel lenses, modifies the beam to increase efficiency and attempt to illuminate the detectors in the same manner as a uniform sky. Light is conveyed by means of liquid light guides from either QTH flat field lamps or a choice of hollow cathode (CuAr, ThAr) and penray (Ar, Hg, Xe, Ne) lamps, used for wavelength calibration. Changing entrance pupil effects are accounted for by employing a moving exit pupil baffle, which can simulate the pupil geometry of a specific track.

Keywords: Segmented mirror telescopes, astronomical instruments, calibrations, diffusers, light guides

1. INTRODUCTION

The Southern African Large Telescope (SALT)^[1], which was completed in November 2005, is currently coming to the end of its commissioning and performance verification phase^[2], which is expected to be concluded by late 2008. Science programs began in 2005 with the installation of the “first light” instruments, the UV-visible imaging camera, SALTICAM, and the imaging spectrograph, RSS (the Robert Stobie Spectrograph). Currently the telescope is typically scheduled ~50-75% of the time for science. The remaining time is allocated to ongoing completion and engineering tasks, mostly involving improvements to the telescope’s image quality performance^[3].

Although the basic design of SALT is very similar to that of the Hobby-Eberly Telescope (HET)^[4], there are significant departures brought about to enhance performance and take advantage of the lessons learned with the HET. A redesigned spherical aberration corrector (SAC)^[5] gives a 4 times larger field of view (8 arcmin diameter) and improved image quality. It also provides the largest entrance pupil (11-m diameter) of any optical telescope yet built, although being under-filled and with a large central obstruction it is effectively equivalent, at best, to a ~8.5 m Cassegrain telescope, and, at worst, to a ~7 m. In addition, by using multi-layer protected Ag/Al coatings^[6] on the four SAC mirrors, SALT’s sensitivity at short wavelengths (<450 nm) has been significantly enhanced, allowing observations down to the atmospheric cut-off (~320 nm). The “first light” UV-visible instruments^[7], an imaging camera (SALTICAM^[8]) and imaging spectrograph (RSS^[9]), are both mounted at prime focus to take advantage of the enhanced blue sensitivity.

Both SALT and HET are optical analogues of the Arecibo radio telescope, where the primary mirror remains stationary during an observation, and objects are tracked by moving a much smaller prime focus payload, containing the SAC and science instruments. Unlike Arecibo, SALT and HET are tilted from the zenith (37° for SALT) to allow for greater sky coverage (~70% of the available sky in the range, namely $-75^\circ < \text{Dec} < +10^\circ$) by rotating the telescope in azimuth for target acquisition. Objects can be observed continuously for periods between ~1 and 3 hours, depending on the declination. While this poses restrictions on target availability and observation times, it is still well matched to the typical exposure and observations times for most astronomical objects, and is well suited to survey science and regular queue scheduled observations, lending a greater flexibility, particularly for synoptic observations. More importantly for

* dibnob@saao.ac.za; SAAO, PO Box 9, Observatory 7935, South Africa; phone +27 21 4606286; fax +27 21 4473639

SALT, it decreased the construction costs by a factor of $5\times - 10\times$ over a conventional telescope, making it far more affordable, particularly for a country like South Africa, and for its SALT partners, with a limited budget. Indeed the final cost of SALT (~\$20M) was closer to a typical 4m class telescope than an 8 – 10m.

The unusual geometries of SALT and HET pose particular difficulties when it comes to calibrating science data. This paper discusses these issues and presents the details of the SALT Calibration System (hereafter referred to as “CalSys”) designed to take account of these various effects. CalSys was installed toward the end of 2005, and has been used successfully to calibrate commissioning data for the first-light instruments, although certain aspects of the calibrations are still to be fully commissioned, which is expected to be concluded later in 2008.

2. SALT PUPIL EFFECTS

Since the SAC moves with respect to the segmented primary mirror array, the entrance pupil moves similarly, resulting in a variation in the illumination of the segments as an object is tracked across the sky. This results in a pupil which “migrates” across the primary. The size and geometry of the pupil is completely determined by the SAC optical design, and particularly the sizes of the SAC mirrors and their central holes. Various alternative SAC designs were considered, with pupil sizes varying from 9 to 16 m in diameter. For a given field size, increased pupil diameters come with increased SAC mirror/hole sizes, which also determine the size of the central obstruction. Deciding on the most appropriate pupil size was determined from a trade-off study, which involved the following:

- Field size
- Effective maximum collecting area
- How collecting area varies with track time
- The size, complexity and cost of the SAC

The final optimal design converged to a SAC with an 11-m diameter entrance pupil provided by mirrors mounted in a “Gregorian-Cassegrain” configuration (Figure 1), the largest being 620 mm in diameter. This provided a good cost-performance compromise and resulting in a $4\times$ larger science area (8 arcmin diameter) and $\sim 15\%$ increase in effective collecting area compared to HET, whose “double-Gregorian” style SAC provided a 9.2 m pupil and a ~ 4 arcmin diameter field of view^[5].

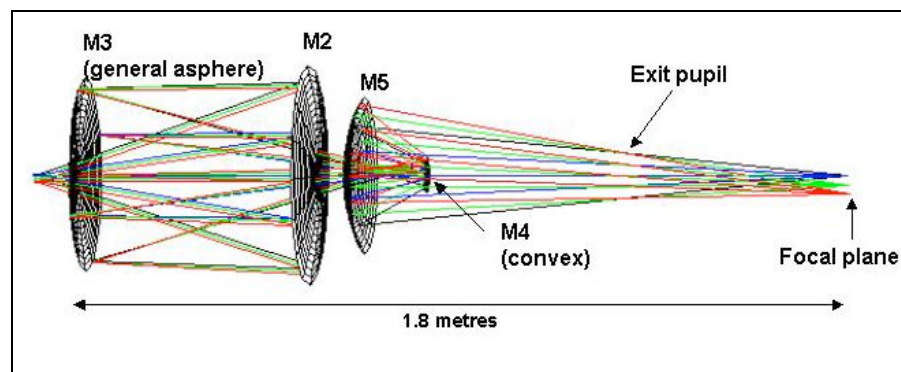


Figure 1: The SALT Spherical Aberration Corrector

The added advantage of the SALT SAC design, apart from its optical properties, is the fact that the back focal distance is considerable (~ 1 m from the last SAC mirror, M4), which allows plenty of room to mount instrumentation at the prime focus. Four focal “stations” are provided: one direct (which feeds RSS), and three with 45° fold mirror (feeding SALTICAM, the future Fibre Instrument Feed and an Auxiliary Focus for small-scale instruments). In addition, the exit pupil is also well separated from the optics, which has an important benefit when it comes to optimally baffling the system. The space between M4 and the exit pupil has also allowed for the introduction of an atmospheric dispersion compensator (ADC)^[10].

In Figure 2 we show how the SALT entrance pupil (in yellow) moves across the primary mirror during an observation, which leads to a time-varying effective area of the primary mirror (Figure 3). The tracker, situated at the prime focus, can move over a $\sim 3.2 \text{ m} \times 3.2 \text{ m}$ area, with a ~ 1.5 tonne payload which carries the SAC and instruments. This payload is mounted on a hexapod platform that allows it to tip/tilt, thereby always keeping the optical axis of the SAC aligned with a spherical primary mirror radius vector. The absolute precision of this alignment is a staggering $\sim 5\mu\text{m}$ in all 6 degrees of freedom, namely x, y, z and the three rotations about these axes (where x & y define the plane enclosing the top hexagonal structure). This is achieved by a position measuring feedback system using both a distance measuring interferometer and autocollimator, both of which optically sense relative motions (axial displacement and tip/tilt, respectively) with respect to the primary mirror array, which is $\sim 13 \text{ m}$ away.

The pupil depicted in Figure 2 is for a point source in the field centre, but for an arbitrary tracker offset. This pupil has an effective central obstruction of $\sim 4.5 \text{ m}$ diameter, resulting in a maximum effective area (taking into account tracker shadowing, mirror segment gaps, chamfers and non-figured/coated corners), when the tracker is centred, of 57.3 m^2 , equivalent to an un-obscured 8.5-m mirror. The size of the pupil just matches the circle circumscribing the mirror array, which is 11-m from corner-to-corner. This implies that light sources outside of the primary mirror array (e.g. scattered Moonlight off the telescope structure, the floor, etc.) could, in principle, end up at the focal plane. For this reason a moving hexagonal mirror baffle, with the same relative geometry as the primary array, is situated at the exit pupil in the prime focus payload. This serves the dual purpose of controlling stray light and is also important for performing accurate calibrations whereby the same pupil geometry as experienced by an on-sky object can be duplicated for a calibration observation (e.g. a flat field or wavelength calibration arc lamp exposure). During an on-sky observation the mirror baffle motion is slaved to the tracker motion to provide continuous baffling of stray light.

An additional complexity is that the exit pupil, which is $\sim 150 \text{ mm}$ in diameter, also undergoes a displacement due to the ADC. This amounts to $\sim 7 \text{ mm}$ over the maximum zenith distance range (1.17 – 1.37). This effect therefore requires the addition of a circular pupil baffle which moves according to the ADC displacement.

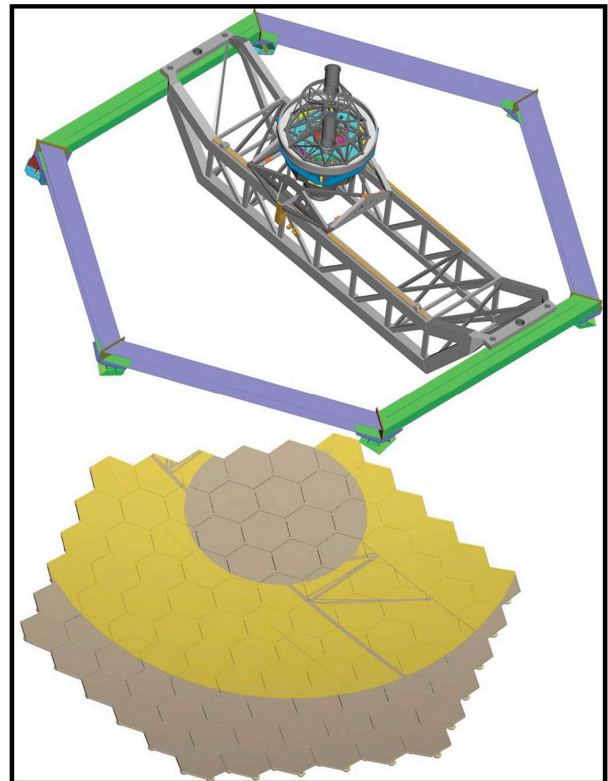


Figure 2: SALT pupil geometry for an on-axis source at an arbitrary tracker position.

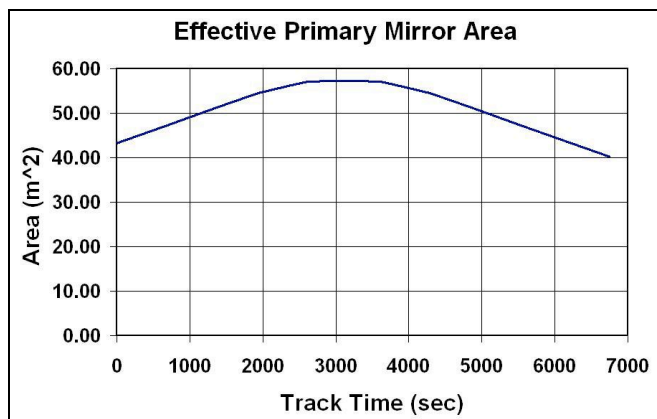


Figure 3: Effective telescope area vs track time at azimuth = 180°

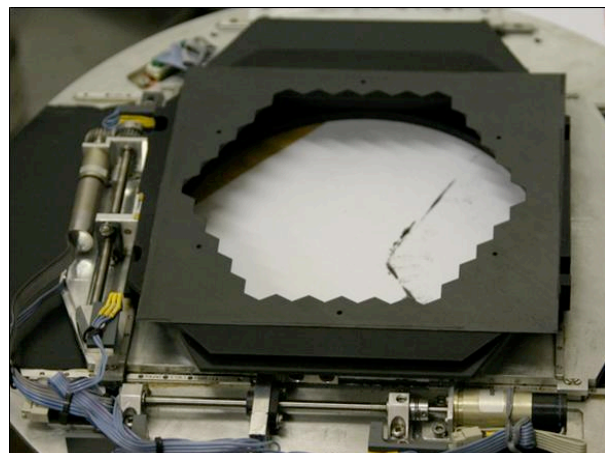


Figure 4: The moving exit pupil baffle.

The variation of the pupil illumination as a function of field angle is shown in Figures 5 & 6 for both centred and maximum off-centre tracker positions, each for six different field angles, from 0 to 5 arcmin off-axis. These variations imply that the ray bundles arriving at the focal plane are modified such that they experience significant asymmetric vignetting.

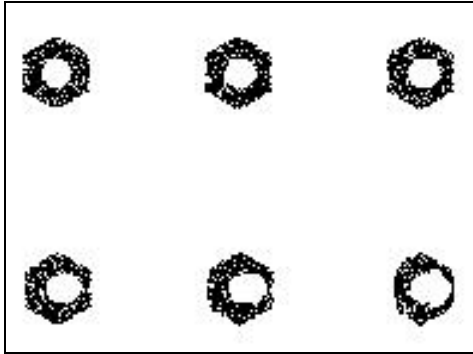


Figure 5: Change in the pupil illumination as a function of field angle for a centred tracker. Top: field angles 0, 1 & 2 arcmin. Bottom row: 3, 4 & 5 arcmin.

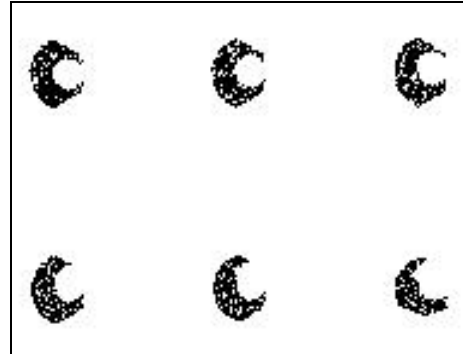


Figure 6: Change in the pupil illumination as a function of field angle for a tracker at maximum x offset of 6° . Top row: field angle 0, 1 & 2 arcmin. Bottom row: 3, 4 & 5 arcmin.

Although the SALT focal plane is flat, there is a variation in telecentricity with field angle, amounting to 5° at a field angle of 4 arcmin, as demonstrated in Figure 7.

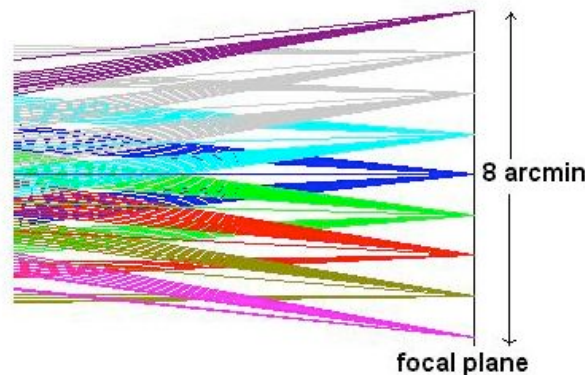


Figure 7: Variation in the telecentric angle with field position.

From the above discussion it is apparent that the far-field SALT images are quite complex and are dependent upon both the tracker position and field angle, as a result of vignetting of rays by the SAC optics and loss of rays from the un-illuminated parts of the entrance pupil.

3. CALIBRATION REQUIREMENTS

Ideal astronomical data calibrations for detectors and instrument sensitivity effects (i.e. “flat-fielding”) are achieved by attempting to simulate, in the calibration observations (e.g. a flat-field), the same illumination conditions as applied for the actual astronomical observation (i.e. on sky). For a “normal” telescope, with a fixed and symmetrical entrance pupil, the job is a lot easier than for the case of the telescope like SALT, with its moving pupil. For flat-fielding out sensitivity variations, from high frequency pixel-to-pixel sensitivity variations to lower frequency effects (e.g. vignetting), it is

usual to attempt to uniformly illuminate the detector, in much the same manner as a uniformly illuminated sky would. Indeed many techniques used with smaller telescopes involve both the use of flat fields derived from (twilight) sky observations and internal calibration lamps. The latter invariably have different illumination patterns compared to the sky, which is often dealt with by correcting the low frequency illumination of a lamp flat-field by normalizing to a smoothed sky illumination.

When it comes to wavelength calibrating SALT spectroscopic data, subtle effects can come into play because of the complex far-field pattern in arc calibration lamp exposures. This might not necessarily result in noticeable PSF shape changes, but nonetheless, the ray bundle structure can be very dependent on field angle and tracker position due to non-telecentricity and asymmetry of the far field. In principle, pupil illumination changes (with time and position) can couple with optical aberrations in instruments to produce detectable shifts in arc lines, particularly at high spectral resolution. For the SALT High Resolution Spectrograph (HRS, currently under construction^[7]) this is somewhat mitigated by the fact that it is fed by an optical fibre, which azimuthally scrambles the light rays, removing most pupil asymmetry effects. However, in an ideal calibration system the light rays should have the same distribution of angles of incidence at the detector as a function of field and tracker position to avoid subtle line centroiding effects.

In designing CalSys the following set of requirements guided the design approach:

- Efficiency, both in terms of throughput and operation
- Flexibility, to allow different types of calibrations to be conducted for a variety of different programs
- Accuracy, in terms of optically designing a system to simulate a uniformly illuminated sky
- To use a moving baffle at the exit pupil to simulate the same pupil filling geometry for the calibration as for the on-sky observation, including time varying effects
- To have the calibration light enter the SAC in the same manner as from the sky and experience the same field dependent vignetting and therefore the same degree of illumination, to within 5%.
- Light from the CalSys must be diffuse and uniform over small scales and such that it has no significant structure which could be imparted on the flat field CCD frames.
- Be capable of calibrating data over the 320 – 900 nm wavelength range with the suite of diffraction gratings in RSS and HRS

To achieve all of the above, CalSys was required to be mounted on the prime focus payload in such a manner that it could inject light into the SAC via the hole in M3 (see Figure 1.). In addition, the light sources also had to be located nearby, since the alternative of having them situated some distance away and feeding light through fused silica optical light guides would be inefficient at short wavelengths.

4. CALIBRATION SYSTEM DESIGN

The final design of CalSys comprised of three major components:

1. the moving baffles located at the exit pupil (Figure 4)
2. a lamp box containing:
 - two quartz tungsten halogen (QTH) flat-field lamps
 - a set of wavelength calibrations lamps:
 - CuAr and ThAr hollow cathode lamps
 - Ne, Ar, Xe and Hg “penray” lamps
 - a variable neutral density filter slide to attenuate flat fields or arcs
 - colour balance filters for boosting relative blue response of flat-fields
 - lenses used to image and concentrate the lamp light into light guides
 - two 3 m long and 8 mm diameter liquid light guides (from Lumatec), optimized for blue (320-500 nm) and red (500-900 nm) wavelengths respectively (see Figure 8).

3. a holographic diffuser screen (from Physical Optics Corp.), coupled with Fresnel lenses, which is illuminated by light from the lamp box light guides and can be inserted and retracted from the SAC entrance hole.

The concept is shown schematically in Figure 9, while the ray tracing from the light guide through the screens and Fresnel lens and into the SAC is shown in Figure 10. The design attempts to mimic the light ray caustics as produced by the spherical primary near the paraxial focus. The diffuser is a light shaping diffuser (LSD), consisting of a UV transmitting acrylic holographic screen which transmits and diffuses light in a highly non-Lambertian manner, such that the light from the screen is mostly confined to a cone of FWHM $\sim 20^\circ$, boosting efficiency. Additional Fresnel lenses attempts to simulate the geometry of the ray caustics near the paraxial focus of M1 (primary), as shown in Figure 10.

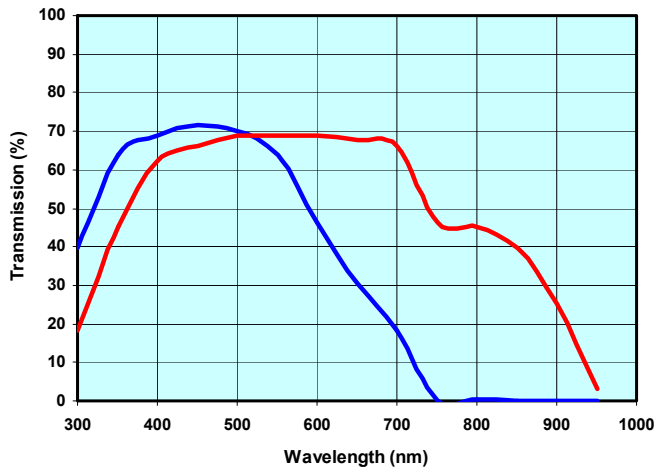


Figure 8: Throughput of the two CalSys liquid light guides.

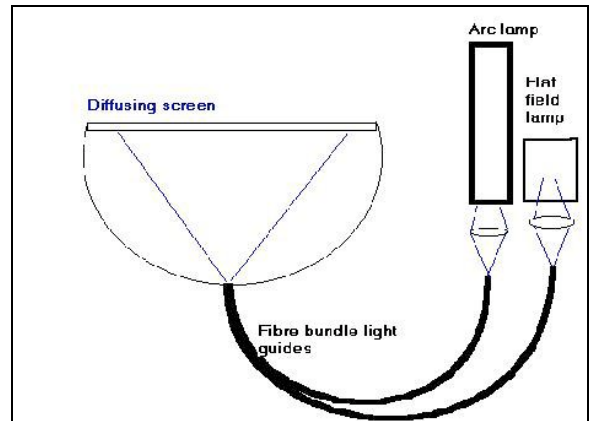


Figure 9: The basic concept of CalSys, which conveys light from sources (flat-field and arc lamps) to a diffuser situated in front of the SAC entrance hole.

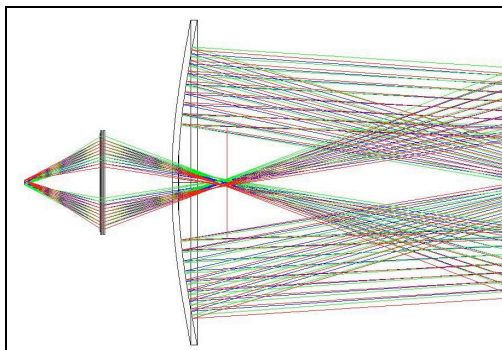


Figure 10: Original concept for CalSys. The light source is the exit face of a light guide (far left), which illuminates a holographic diffuser/Fresnel lens “sandwich”, situated close to the entrance to the SAC (i.e. hole in M3). This arrangement attempts to simulate the caustics near the paraxial focus of M1 (primary mirror). The final design included an additional diffuser to remove structure.

In designing CalSys we also considered using an integrating sphere, but this solution was problematic due to its larger size, weight and inefficiency. An alternative design, based on the integrating concentrator – a modified integrating sphere – developed for the Gemini and SOAR calibration systems^{[11].Error! Reference source not found.}, was also investigated. This system projects a converging beam from a lamp to a small convex mirror on the inside of the spherical reflecting surface of the concentrator. This mirror directs light onto a diffusing screen at the centre of curvature of the concentrator. Light from the diffusing screen produces a uniformly illuminated beam at the exit hole of the concentrator, which acts as a field stop. The f /ratio of the exit beam is governed by the distance of the exit hole from the diffuser screen, and the size of the hole. The interior of the concentrator is a highly polished spherical surface, which returns any light failing to exit on the first pass back to the diffuser. This makes for a very efficient system, much more so than a normal integrating sphere. However, this design was not well suited to the SALT requirement for a small light-weight deployable system. A fibre back-light screen was also considered, but this exhibited too much structure. The current design, based on diffusers and Fresnel lenses, was considered to be adequate in terms of the requirements.

5. PREDICTED PERFORMANCE

During the design process simulations of the CalSys performance was carried out using Zemax, using macros, and Matlab, in order to predict the nature of the illumination patterns in the pupil and focal planes and the angles of incidence of rays arriving at the focal plane over all field angles. In Figure 11 we show a contour diagram which compares the distribution of the angles of incidence for a uniformly illuminated sky and CalSys for different field angles, which are closely matched. The field averaged incidence angles are also compared in Figure 12.

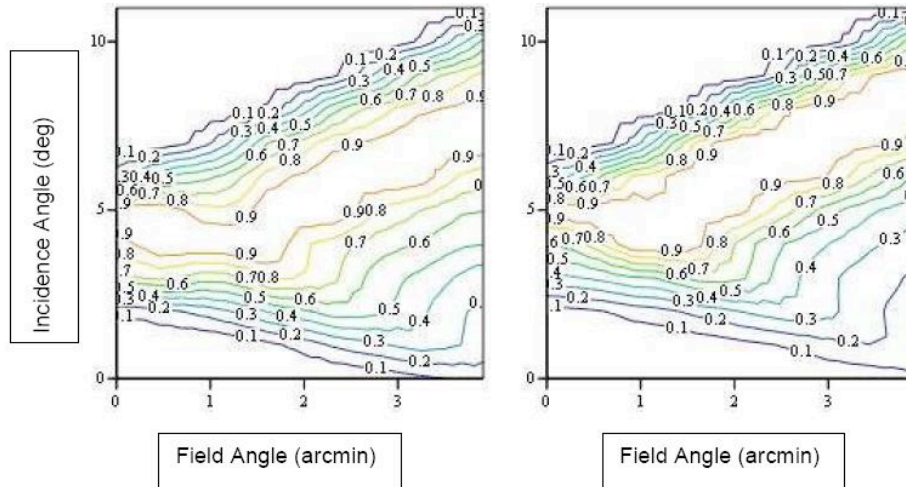


Figure 11: A map of the distribution of angles of incidence of un-vignetted rays arriving at the focal plane as a function of field angle for a uniformly illuminated sky (left) and from the CalSys screen (right). The contours are the fractional distributions, normalized to the most common incidence angle.

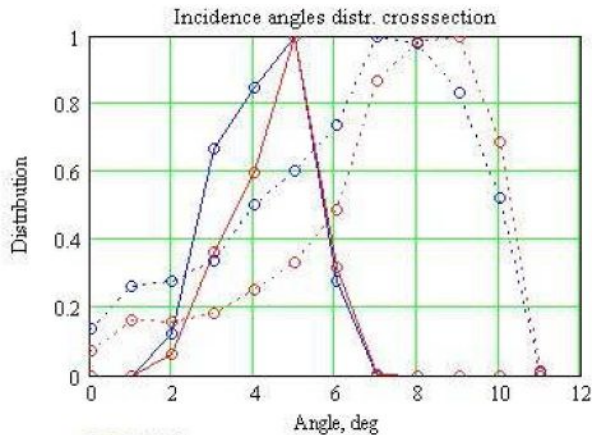


Figure 12: Distributions of ray bundle incidence angles for two field angles: a.) on-axis (solid lines) and, b.) 4 arcmin off-axis (dotted lines). Blue lines refer to the uniform sky reference, and red lines are for CalSys. The two sets of curves are therefore vertical cuts of Figure 11 at $x = 0$ and 4 arcmin, respectively.

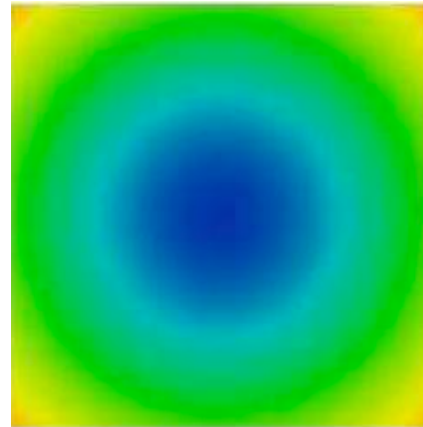


Figure 13: A map of the 8×8 arcmin focal plane which represents the *average* angle of incidence of unvignetted rays arriving at the focal plane, which varies from $\sim 5^\circ$ (blue) for $\sim 0 - 3$ arcmin (on axis), $\sim 7^\circ$ (green) at $\sim 3 - 5$ arcmin, through to $\sim 9^\circ$ at >5 arcmin (corners).

These simulations indicate that the design requirement, in terms of CalSys angles of incidence, to closely simulate a uniformly illuminated sky is met both for a centred tracker (symmetrical pupil) and for random tracker positions (asymmetrical pupil). An example of mean incidence angles variation for the tracker at it maximum offset is shown in Figure 14.

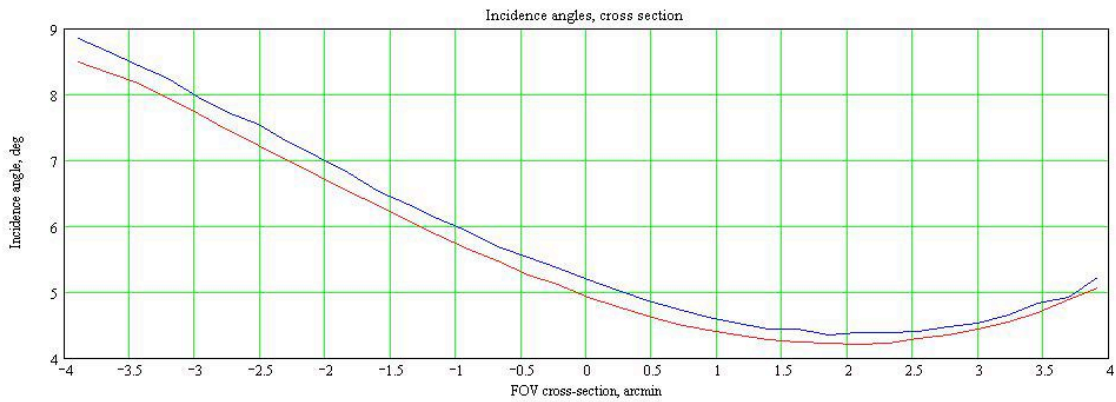


Figure 14: The mean angles of incidence at the focal plane of unvignetted rays as a function of field angle for the maximum tracker off-set of 6°. Upper curve (blue) is for the illuminated sky while lower curve (red) is for CalSys.

Simulations for the sky and CalSys were also made of the pupil and focal plane illuminations, as a function of tracker angle. For the latter we find that the CalSys illumination falls off somewhat steeply with field angle than for the sky illumination, by a constant of 6-10%, for most tracker positions. This is a departure from the calibration specification (~5%), although this is not considered to be too significant since it can be corrected using a library of master sky flat-fields to remove the effect.

The exit pupil baffle will ensure that only rays coming from the part of the primary mirror inside the entrance pupil will arrive at the focal plane. As mentioned already, this baffle will also stop scattered light from outside of the pupil, or primary mirror segments not inside the pupil, from contaminating the signal. For calibration observations, the exit pupil baffle is crucial in simulating the same degree of pupil filling as the on-sky observations. The comparison of pupil illumination patterns is shown below. For a point source, the pupil illumination would be uniform. The simulation of an evenly illuminated sky is achieved by having a large number of point sources of uniform density on the sky. Because off-axis sources are vignetted by the SAC optics, the resultant pupil illumination from all of these sources is not uniform, as can be seen in the figure below.

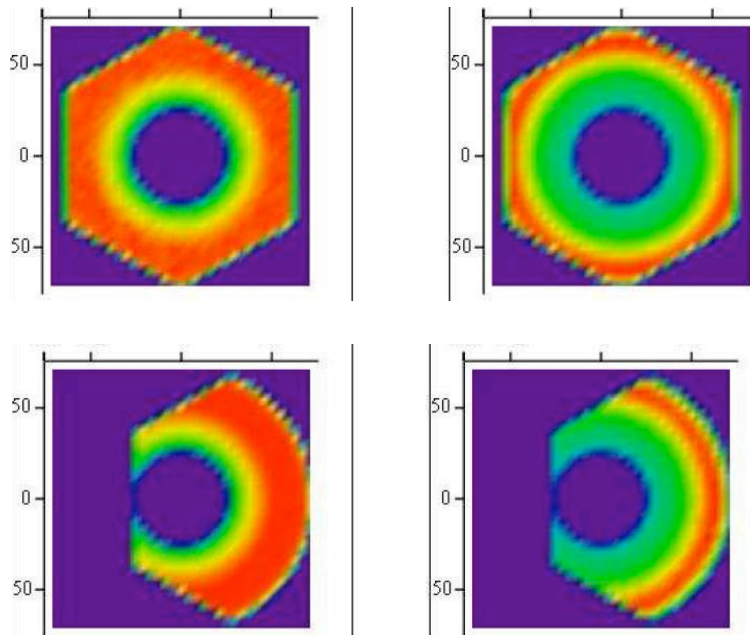


Figure 15: The mean illumination of the exit pupil, from all field angles (0 to 4 arcmin), for (left) uniformly illuminated sky and (right) CalSys for tracker position at 0° (top) and 6° (maximum x-offset).

From our model simulations, the predicted characteristics of CalSys broadly meets the requirements set out in §3, although the illumination of the pupil is a little more peaked in CalSys than for a uniform sky and the vignetting a little more severe at the edge of the field. However, neither of these departures is considered to have a deleterious effect on the performance of the calibration system in terms of adequately flat-fielding CCD data. Similarly, the CalSys wavelength calibration is expected to meet the requirements for the existing (RSS) and future spectrographs (HRS).

6. THE AS-BUILT CALSYS

The final mechanical design for CalSys “screen” was modified by adding a second diffuser, mostly to remove structure in the far field produced by the Fresnel lens, and a schematic is shown in Figure 16. This had little effect on the predicted performance, which was subsequently confirmed by experimentation. The illuminating liquid light guides are attached at the bottom of the structure and include a 60:40 beamsplitter, optimized to allow transmission of red light and reflection of blue light. Thus the red light guide is mounted on-axis while the blue light guide is attached at 90° to the optical axis. The entire structure is wrapped in light-tight black baffling material and is mounted on a on an articulation system which can swing the screen into the beam, in front of the SAC (see photo in Figure 17).

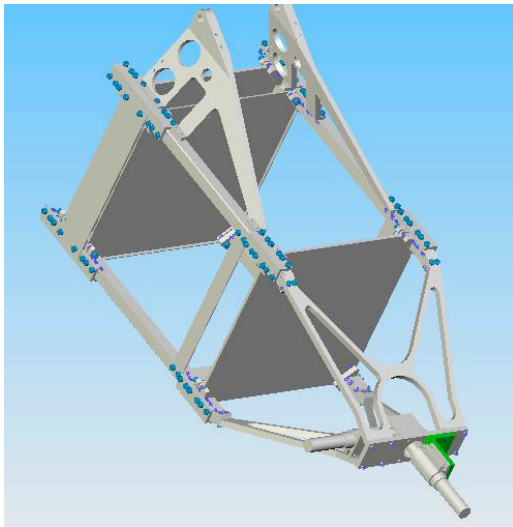


Figure 16: Schematic of the CalSys “screen”, which contain both diffuser screens (top and bottom) and a Fresnel lens (below the top diffuser). The red and blue liquid light guides attach to the bottom and are fed directly (red) or by a beamsplitter (blue).

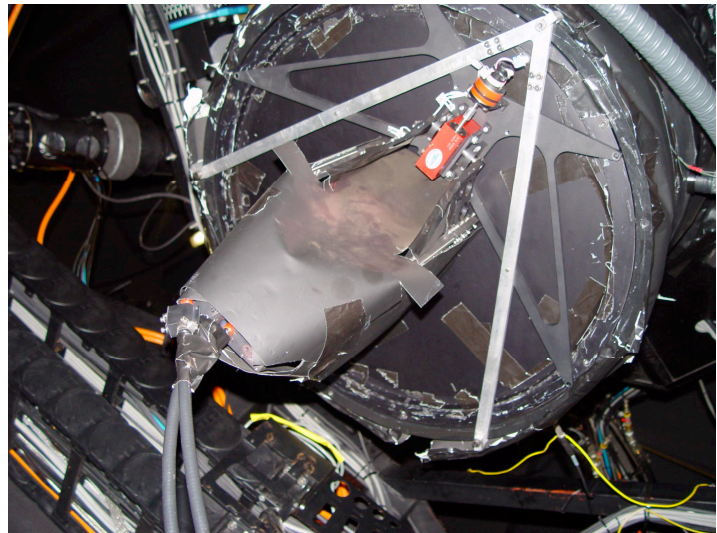


Figure 17: A photo of the CalSys screen deployed into position below the SAC. The two liquid light guides can be seen exiting the bottom, while the actuator is seen inside the apex of the triangular supporting struts.

The lamp box structure is shown in Figure 18, which compactly mounts the two hollow cathode lamps, four Penray lamps and two QTH lamps (not shown). In addition each lamp has its own lenses, which are mounted into a plate with appropriate holes (seen in the centre), to focus the light into the light guides. A colour filter wheel for both the QTH lamps allows the spectral distribution to be modified to boost relative output in the blue, for spectral observations in this region. A linearly variable neutral density filter slide, which can be used to attenuate both QTH and arc lamp exposures by up to a factor of 100×, can be seen below the lens holder plate.

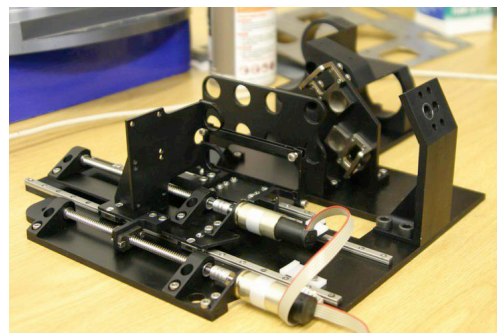


Figure 18: The unpopulated lamp-box chassis.

The two light guides (not shown) are mounted onto two independent translation stages which allow each of them to access up to four different lamps, grouped into “blue” (CuAr, Ar, Hg(Ar) & QTH) and “red” (ThAr, Xe, Ne & QTH) types, depending on which spectral region they are best suited for. The beamsplitter in the CalSys screen subsystem allows both light guides to be used simultaneously, so that arc lines from different lamps can be mixed, if desired, potentially providing more choice for wavelength calibration lines. The lamp box is mounted onto the Prime Focus Payload in a dedicated bay, which will eventually be cooled by a glycol heat exchanger. Power supplies for all of the lamps are mounted inside a separate cooled electronics box mounted on the telescope structure. The cable length for the lamps is ~ 20 m.

CalSys was installed on SALT in late 2005, in time to support the early commissioning of RSS. It has performed to specification in terms of efficiency and operation. In fact an additional ND filter was installed, primarily for the flat-field QTH lamps, since they were too bright for certain instrument configurations. The measured flat-field illumination using CalSys is close to the model prediction, with a steeper fall off with field angle. One puzzle, however, was that the vignetting for the sky was different than predicted, having a more peaked distribution and a smoother roll off towards the edge of the field, resulting in more vignetting. The cause of this was subsequently traced to a diaphragm in the SAC for which the central hole was sized too small, something that will be modified soon. Because of ongoing investigations into SALT’s image quality^[3], which has also stalled commissioning of the ADC and moving exit pupil baffles, final commissioning of CalSys has had to be delayed. However, we have already successfully used CalSys to calibrate data obtained with a variety of RSS modes and we are satisfied that it is performing as expected and will meet its design specifications.

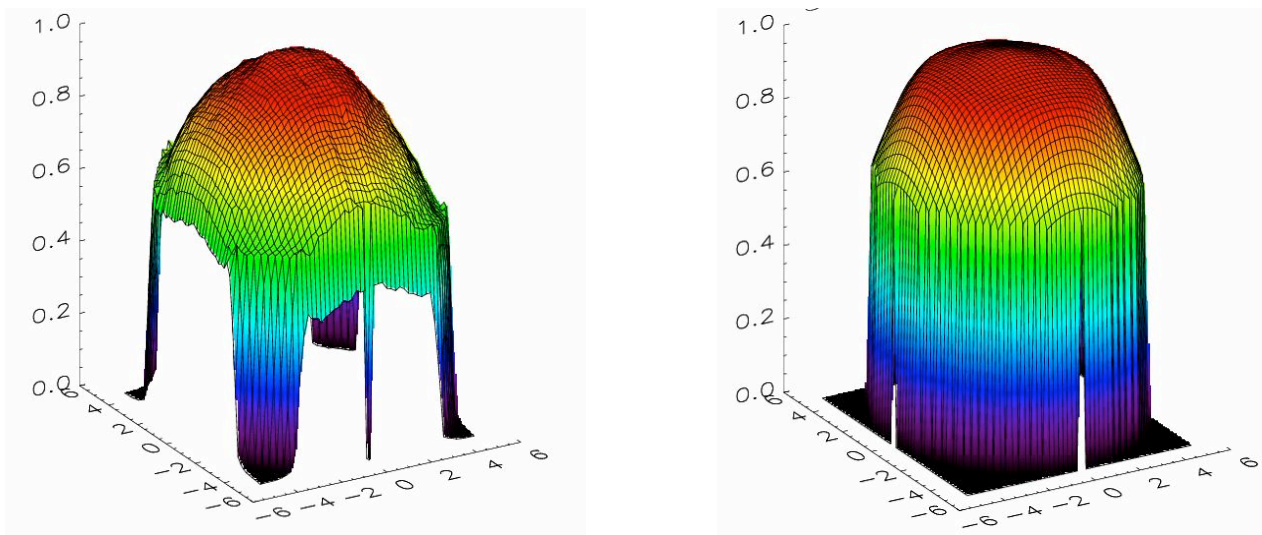


Figure 19: Comparison between the observed (left) and predicted (right) sky flat-field illumination in the focal plane. The difference is due to increased SAC vignetting (see text).

7. SUMMARY

This paper has described the somewhat unusual requirements for calibrating SALT data and the design and development of the SALT calibration system, CalSys. The system is designed to support to calibrations of the SALT first-generation instruments and their various modes over the full 320-900 nm wavelength range that they cover. These include both flat-field and wavelength calibrations. CalSys has been designed to take account of the variable and time dependent vignetting of both the exit pupil and focal plane. The former will be dealt with by used a moving baffle to simulate pupil filling experienced on-sky. The eventual complete calibration procedure will involve using CalSys to “replay” tracker trajectories with the exit pupil mirror baffle during a calibration observations, which will automatically be done following the night’s observations. The SALT science database records the tracker trajectories and this

information will then be used by the automated CalSys program. We expect that CalSys will support more exacting calibrations that might require identical pupil geometries and vignetting effects for both on-sky and calibration observations. CalSys was designed and built in-house using both COTS equipment (light guides, screens, lamps, lenses, filters) together with custom designed components, namely the lamp box, deployable screen and pupil baffle(s).

ACKNOWLEDGMENTS

Much of the original mechanical design for CalSys was carried out by Willem Esterhuysen and Faried Ebrahim while SALT Operations and SAAO technical staff assisted with the installation and commissioning of CalSys.

REFERENCES

- [1] Buckley, D.A.H., Swart, G. P. and Meiring, J.G., "Completion and Commissioning of the Southern African Large Telescope," *Proc. SPIE* **6267**, 62670Z (2006).
- [2] Buckley, D.A.H., et al., "Commissioning of the SALT First Generation Instruments," *Proc. SPIE* **7014**, these proceedings (2008).
- [3] O'Donoghue, D., et al., "The image quality of the Southern African Large Telescope," *Proc. SPIE* **7018**, these proceedings (2008).
- [4] Ramsey, L. W., et al., "The early performance and present status of the Hobby-Eberly telescope," *Proc. SPIE* **3352**, 34 (1998).
- [5] O'Donoghue, D. and Swat, A., "The Spherical Aberration Corrector for the SALT," *Proc. SPIE* **4411**, 72 (2001).
- [6] Wolfe, J., Sanders, D., Bryan, S. and Thomas, N., "Deposition of durable wide-band silver mirror coatings using long-throw, low-pressure, DC-pulsed magnetron sputtering," *Proc. SPIE* **4842**, 343 (2003).
- [7] Buckley, D.A.H., et al., "Status of the SALT First Generation Instruments," *Proc. SPIE* **6269**, 62690A (2006).
- [8] O'Donoghue, D., et al. "SALTICAM: a \$0.5M acquisition Camera: Every Big Telescope Should Have One," *Proc. SPIE* **4841**, 465 (2003).
- [9] Burgh, E., et al., "The Prime Focus Imaging Spectrograph for the Southern African Large Telescope: optical design," *Proc. SPIE* **4841**, 1463 (2003).
- [10] O'Donoghue, D., "The Atmospheric Dispersion Corrector for SALT," *Proc. SPIE* **4411**, 79 (2001).
- [11] Ramsay-Howat, S. K., Harris, J. W. and Bennett, R. J., "Dedicated Calibration Facility for the Gemini Telescopes," *Proc. SPIE* **2871**, 1171 (1997).
- [12] Ramsay-Howat, S. K., et al., "Gemini Facility Calibrations Unit," *Proc. SPIE* **4008**, 1351 (2000).